Appl. Phys. A 70, 145–151 (2000) / Digital Object Identifier (DOI) 10.1007/s003390000253

Applied Physics A
Materials
Science & Processing

Single-walled carbon nanotubes produced by cw CO_2-laser ablation: study of parameters important for their formation

E. Muñoz[1], W.K. Maser[1,*], A.M. Benito[1], M.T. Martínez[1], G.F. de la Fuente[2], A. Righi[3], J.L. Sauvajol[3], E. Anglaret[3], Y. Maniette[4]

[1] Instituto de Carboquímica (CSIC), María de Luna 12, 50015 Zaragoza, Spain
(Fax: +34-976/733-318)
[2] Laboratorio de Procesado de Materiales por Láser, Instituto de Ciencia de Materiales de Aragón (CSIC-Universidad de Zaragoza), María de Luna 3, 50015 Zaragoza, Spain
[3] Groupe de Dynamique des Phases Condensées, Université de Montpellier II, Place E. Bataillon, 34095 Montpellier Cedex, France
[4] Serveis Científico-Tècnics, Secció Caracterització Materials, Universitat de Barcelona, Lluís Solé i Sabarís 1-3, 08028 Barcelona, Spain

Received: 29 June 1999/Accepted: 8 September 1999/Published online: 21 January 2000 –

Abstract. The production of single-walled carbon nanotubes (SWNTs) using the cw CO_2-laser ablation technique is reported. Different metals and metal concentrations in the carbon targets as well as different buffer gases and gas pressures have been used in order to study their influence on the formation of SWNTs. It is shown that the conditions near the evaporation zone, i.e. especially the local temperature environment induced by the laser radiation as well as the used metals play a key role in the formation process of SWNTs. Employing a very simple experimental setup the cw CO_2-laser ablation technique easily provides the environment favorable for the growth of high quality SWNT material under a wide range of experimental conditions.

PACS: 81.05.Tp; 81.10.Bk; 61.48.+c

There is a large variety of potential applications of single-walled carbon nanotubes (SWNTs) forming a highly diversified technology portfolio ranging from nano-electronics [1, 2] to material science [3] and fuel-cell technology [4]. A crucial point for further progress in the exploitation of their properties and their applications certainly is the production of high-quality nanotubes with defined properties in large quantities in a cheap and reliable way. Here, great progress has been made using the electric arc-discharge method as a batch process [5], and the laser ablation technique using double-pulsed laser-furnace configurations, as a continuous way of production [6, 7]. Recently our group has shown that a typical industrial CO_2-laser system working in continuous wave (cw) mode can also be efficiently used for the production of SWNTs [8]. Combining this laser system with a very simple evaporation setup, this not only is a step towards industrial mass production but also will lead to a better understanding of the role of various parameters for the formation of SWNTs [9].

This article describes in detail the production of SWNTs using this CO_2-laser system operating in cw mode. The influence of parameters such as the composition of the graphite/metal targets, the buffer gas, its flow rate, and its pressure on the formation of SWNTs are discussed. The results reveal that most of the parameters have a strong influence on the temperature environment close to the target rod. Here, the local temperature conditions as well as the used metals play an essential role for the growth of the SWNTs.

1 Experimental

The production of SWNTs was achieved using a CO_2 laser operating in continuous wave mode at 10.6 μm. The laser beam was focused onto a graphite/metal-composite target (spot size: 0.8 mm^2, power density: 12 kW/cm^2) placed inside a stainless steel evaporation chamber (Fig. 1) of ≈ 7 liters in volume. Cylindrical targets of 5.5–6 mm in diameter were prepared by compacting homogeneous mixtures of powdered graphite and metals in an isostatic press. No further heat treatment has been applied to the target rods. The following metal concentrations (in at%) were used in the present work: Ni (2), Co (2), Y (0.5), Fe (2), Ni/Co (4.2/1, 2/2, 2/0.5, 1/0.25, 0.6/0.6, 0.5/0.13), Ni/Y (4.2/1, 2/0.5, 1/0.25, 0.6/0.6, 0.5/0.13), Ni/Fe (4.2/1, 2/0.5, 0.6/0.6), Co/Y (2/0.5), and Ni/La (2/0.5, using a mixture of Ni and $LaCl_3$). Argon, nitrogen, and helium were employed as buffer gases. Experiments were performed at 400 Torr under both, dynamic (establishing a gas flow of ≈ 1 l/min) and static (without any gas flow) conditions. A detailed study of the effects of using argon or nitrogen as ambient gases in the production of SWNTs was carried out by laser ablation of Ni/Y (4.2/1) targets under static atmospheres ranging from 50 to 500 Torr.

Figure 1 shows the experimental set-up employed in the present work. During the laser ablation process the targets were continuously rotated around their axis and moved up- and downwards in order to get an uniform evaporation of the target (see also scanning conditions in [9]). With the purpose of maintaining a continuous vaporization, the mirrors, which guide and focus the laser radiation, are cleaned after typical running times of about 15 min. Up to 200 mg of the targets

*Corresponding author. (E-mail: wmaser@carbon.icb.csic.es)

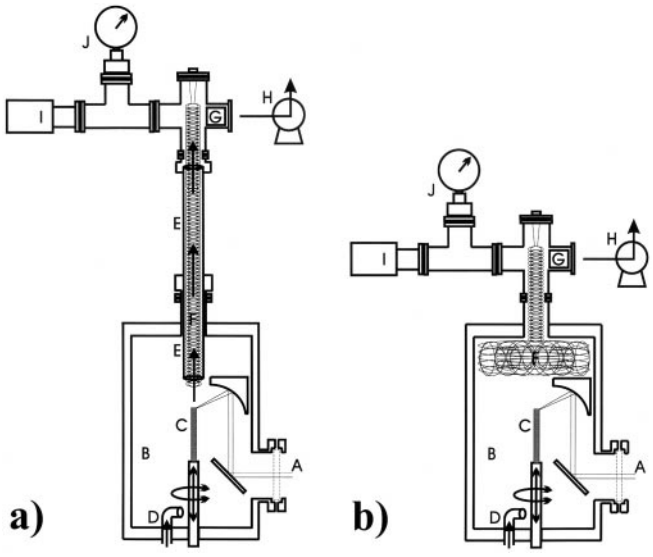

Fig. 1a,b. Experimental setup of the cw CO_2-laser ablation system under dynamic **a** and static **b** conditions. **a** The CO_2-laser radiation (A) is guided into the evaporation chamber (B) and focused onto the graphite/metal-composite target (C), which is rotated and moved up- and downwards to get its uniform evaporation. Gases are introduced into the chamber through a nozzle (D). The pressure and the flow rate were controlled by a pump (H) a Pirani (I), a manometer (J), and a flowmeter. **a** Under dynamic conditions, the gases and the synthesized products are driven through a quartz tube (E) where they can be collected mainly on the copper wire systems (F). Some soot can also be found in the filter (G), as well as on the chamber walls. **b** Under static conditions no quartz tube was used and a copper wire system additionally was placed in the upper part of the chamber in order to increase the condensing surface for SWNT material close to the evaporation zone

were consumed after operation times of 1 h. In the experiments performed using flowing buffer gases (Fig. 1a) most of the synthesized soot was swept inside a quartz tube placed above the target and at the top of the evaporation chamber, and collected mainly on an entangled copper wire and on a filter placed at the end of the quartz tube. The rest of the soot was collected on the chamber walls, as well as on the surface of the quartz tube. The vaporization apparatus employed in the experiments carried out under static atmospheres can be seen in Fig. 1b. Here, the quartz tube was removed and a copper wire system filling the upper part of the evaporation chamber was introduced, thus increasing the collecting surface for the produced materials close to the target.

No further purification process was applied and the as-produced carbonaceous materials have been characterized by scanning electron microscopy (SEM) (JEOL JSM-6400), transmission electron microscopy (TEM) and energy dispersive spectroscopy (Philips CM30, 300 kV), and micro-Raman spectroscopy (argon-ion laser with $\lambda_{exc} = 514.5$ nm, power density (50 mW/mm^2), collection: Jobin-Yvon T6400 spectrometer, resolution $= 2$ cm^{-1}).

2 Results and discussion

2.1 Influence of the target composition

The results presented in this section refer to the experiments carried out under both static and dynamic argon and nitrogen atmospheres at 400 Torr. When targets containing only simple metals were evaporated, the synthesized carbonaceous materials were found in the form of powder-like soot. Occasionally, soot in the form of thin and tiny filaments (less than 1 cm in length) appeared on the copper wire systems when employing Ni or Co. This situation changed drastically, using bi-metallic mixtures. Here, the produced carbonaceous material was collected on the entangled copper wire systems in the form of filamentous soot exhibiting a web-like appearance (Fig. 2). Some of the soot collected on the chamber walls was also in the form of these thin filaments. On the other hand, most of the soot collected on the chamber walls, on the surface of the quartz tube, and in the filter was in the form of a powder-like soot exhibiting a rubbery texture, and sometimes as a thick film [8]. The amount of the web-like filaments was very abundant employing the bi-metallic mixtures mentioned above. Substantially lower amounts only were found using the graphite/bi-metal targets containing the lowest metal concentrations (Ni/Y (0.5/0.13) and Ni/Co (1/0.25, 0.5/0.13)), as well as using the Co/Y mixture.

Both SEM (Fig. 3) and low-magnification TEM (Fig. 4a) images of the web-like material synthesized ablating graph-

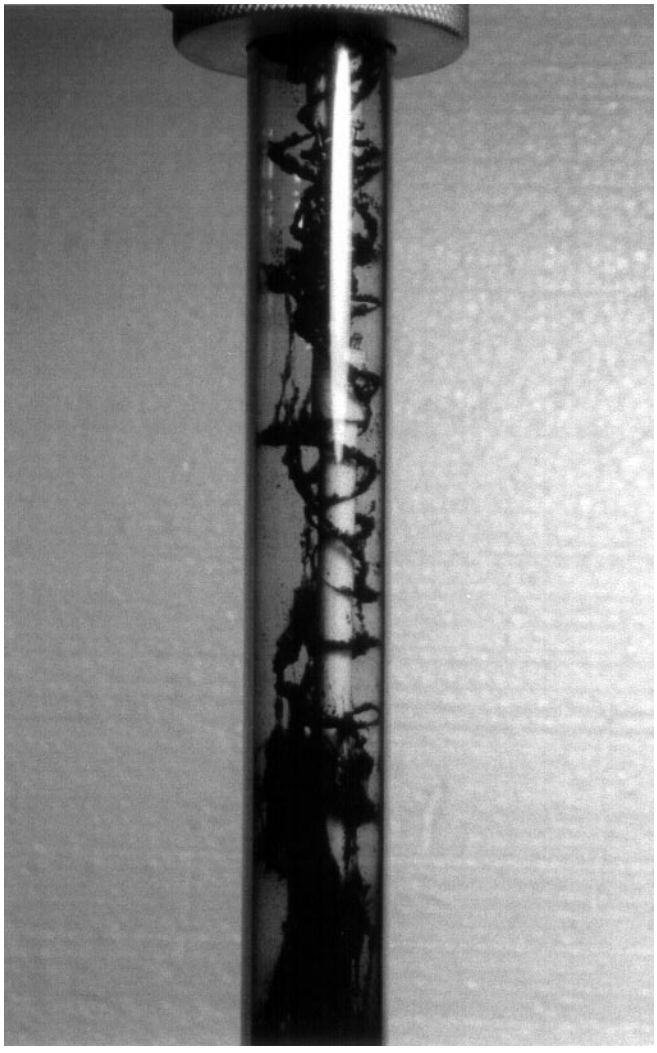

Fig. 2. Web-like soot sticking on the copper wire inside the quartz-tube on top of the evaporation chamber. This aspect is typical for soot material containing high yields of SWNTs

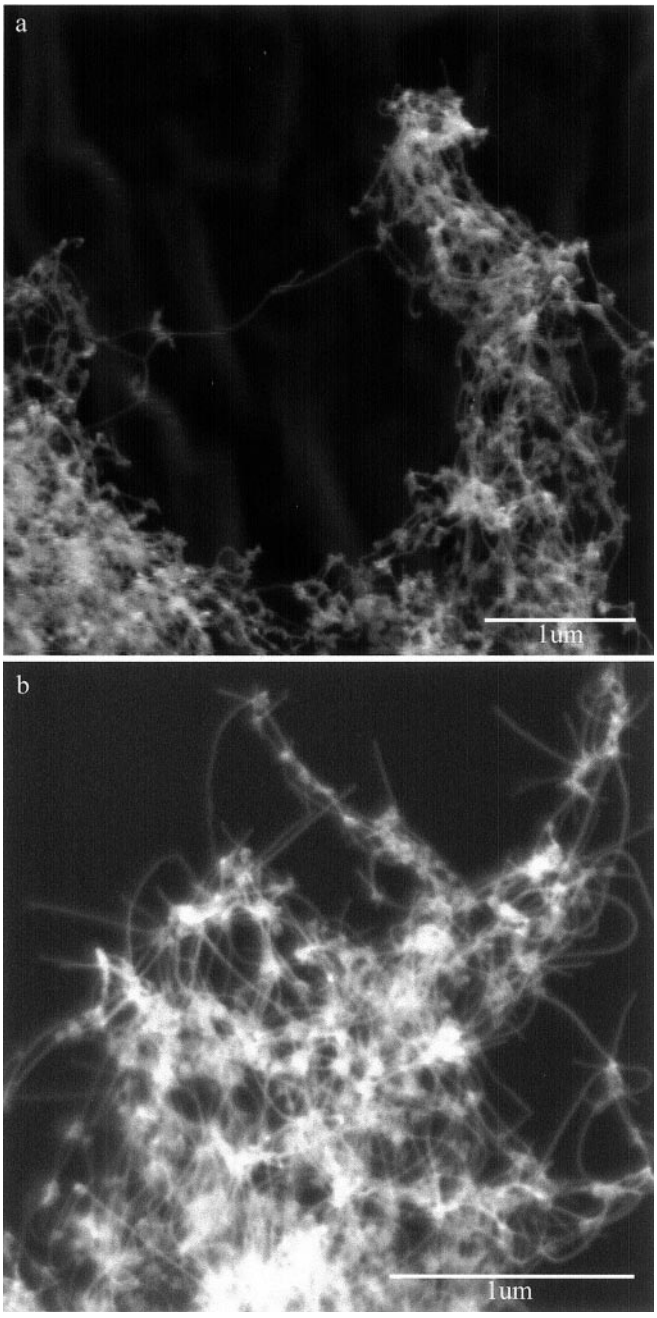

Fig. 3a,b. SEM micrographs of SWNT material produced by laser ablation of a Ni/Y (4.2/1) target under **a** flowing argon and **b** static argon atmospheres at 400 Torr

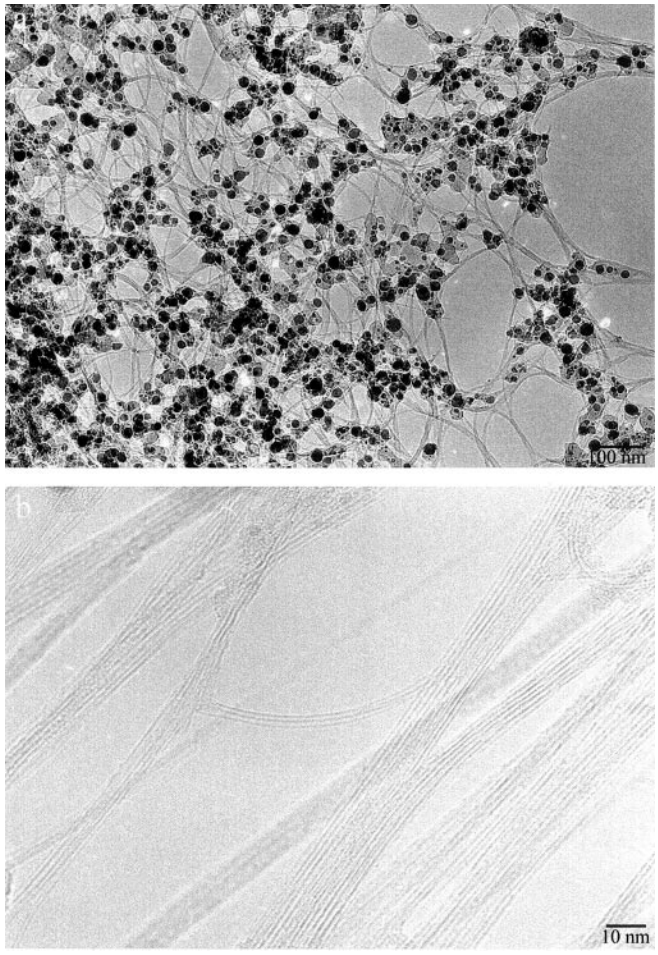

Fig. 4a,b. TEM micrographs of bundles of SWNTs synthesized under static nitrogen atmospheres at 400 Torr using **a** Ni/Y (4.2/1) and **b** Ni/Co (0.6/0.6) targets

ite/bi-metal targets reveal that they contain high densities of entangled carbon filaments of some tens of nm in diameter, more or less homogeneously distributed. Yields of these filaments up to 80 vol% (with respect to the total carbonaceous material) have been estimated from general overviews of the samples observed by SEM and TEM, as those shown in Figs. 3 and 4a. [8]. Particularly high were the densities in SWNT material synthesized using the Ni/Y (4.2/1) mixture, followed by Ni/Y (2/0.5) and then Ni/Co (2/2). Together with these carbon filaments, particles of 5 to 25 nm in diameter having a darker contrast and usually embedded in amorphous carbon can also be seen (Fig. 4a). Electron dispersive spectroscopy on zones containing these particles reveals the presence of the employed metals. In the case of the samples produced using the bi-metallic mixtures, both elements can be found in each particle. However, when using the Ni/Y mixtures, the intensity ratios between the two elements can drastically vary depending on the size of the particle. Here, it was observed that the smaller particles consist almost exclusively of nickel, whereas the largest ones seem to be composed of comparable amounts of both, nickel and yttrium. High-resolution TEM images (Fig. 4b) show that the carbon filaments are in fact SWNTs self-organized into bundles up to 20 nm in diameter. The diameter of individual SWNTs within the bundles is about 1.4 nm, as has been calculated from the fringe spacing or estimated from bundle cross-sections [8]. The bundles, whose extremities are difficult to find by electron microscopy techniques, have lengths in the order of 1 μm, according to recent atomic force microscopy measurements performed on these samples [10]. In contrast to the materials synthesized using bi-metallic mixtures low yields of SWNTs were formed (mainly isolated SWNTs or thin bundles of SWNTs passing through large areas of amorphous carbon) using Ni or Co, whereas no SWNT material was found at all in the samples produced ablating Fe- or Y-containing graphite targets. However, since bi-metallic mixtures such as Ni/Y, Ni/Co, and Ni/Fe drastically enhance the production

of bundles of SWNTs, there seems to be a great synergism in combining certain kind of metals. This effect also has been observed in other production techniques [5, 11]. Furthermore it is important to note that no SWNTs have been observed using pure graphite targets. Therefore, metal particles play a crucial role in the formation process of SWNTs. Although some attempts have been done to explain the role of the metal particles [6, 12] the microscopic details for the growth mechanism and for the synergetic enhancement effect still remain unclear.

More detailed information concerning the influence of the target composition on the structural characteristics of the produced SWNTs as well as on the sample quality can be obtained by Raman spectroscopy. In the low-frequency part of the spectra between 130 and 210 cm^{-1} a broad band consisting of eight to nine peaks can be observed which clearly indicates the presence of SWNTs (Fig. 5). Since every peak in this region corresponds to a characteristic diameter of SWNTs (calculated from the relation provided by Bandow et al. [13] $d(\mathrm{nm}) = 223.75/\nu_{\mathrm{peak}}(\mathrm{cm}^{-1})$) one typically can observe distributions of diameters ranging from 1.1 to 1.6 nm, consistent with the results of TEM. In general, the contribution of the large-diameter tubes is more important in samples synthesized using Ni/Y mixtures (Fig. 5b), and it is especially significant in the samples produced with the Co/Y mixture (Fig. 5f). Here, the most intense peaks are located between 140 and 145 cm^{-1}, which correspond to tubes of about 1.6 nm in diameter. It is also worth mentioning the important contribution of the small-diameter tubes (band at $\approx 202\ cm^{-1}$ corresponding to diameters of about 1.1 nm) observed in the samples produced using the Ni/La mixture (Fig. 5e). Therefore, it seems that certain metals or metal combinations in the production process can cause a significant change of the most pronounced diameter within the typical SWNT diameter distribution. However, no correlation between the target composition and the dominance of certain kind of chiralities within the SWNT samples could be established analyzing the frequency region between 700 and 1000 cm^{-1} which is sensitive to the different kinds of chiralities of SWNT [14].

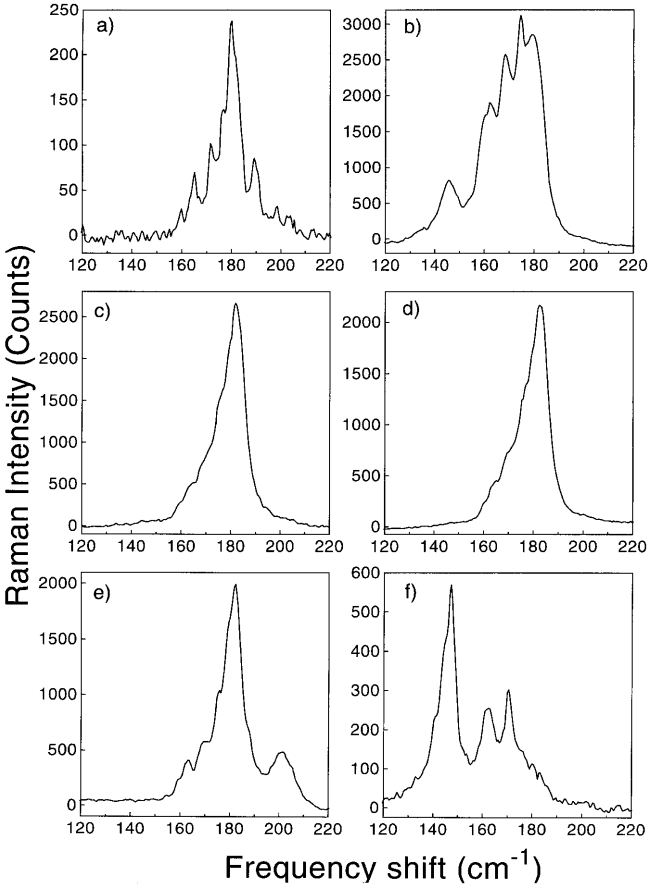

Fig. 5a–f. Low-frequency regions of the Raman spectra ($\lambda_{\mathrm{exc}} = 514.5$ nm) of SWNTs produced using different metal compositions (in at%): **a** Ni (2), **b** Ni/Y (0.6/0.6), **c** Ni/Co (0.6/0.6), **d** Ni/Fe (2/0.5), **e** Ni/La (2/0.5), and **f** Co/Y (2/0.5). All these samples were produced in dynamic conditions using argon atmospheres at 400 Torr

Since the intensities of the low-frequency bands are closely related to the content of SWNTs in the samples one can derive from the signal in this region some information about the quality of the materials. Comparing the intensities of the various spectra shown in Fig. 5, the highest amount of SWNTs within the sample can be assigned in general to samples prepared with Ni/Y mixtures followed closely by Ni/Co, and then Ni/Fe and Ni/La target compositions. Furthermore, the study of the band around 1350 cm^{-1} which is characteristic for disordered carbon reveals that the samples with the highest SWNTs amount (Ni/Y and Ni/Co) contain as well the lowest content of amorphous carbon. However, Ni/La samples as well as bi-metallic samples that yielded the lowest amounts of web-like soot show higher contents of amorphous carbon. Finally, samples synthesized with targets containing only one metal reveal a low SWNT content and the dominance of amorphous carbon. All these Raman results are consistent with the observations from electron microscopy.

Altogether, metals have a strong influence on the production of SWNTs. This concerns especially their quantity but as well their individual characteristics, particularly their diameter distribution. Whereas Ni/Y and Ni/Co mixtures have been established to produce the largest amounts of high-quality SWNT material, no clear correlation of the target composition to the structural characteristics of individual SWNTs (diameter and chirality) could be found.

2.2 Influence of buffer gas and gas pressure

The results presented in this section refer to the experiments carried out using the favorable Ni/Y (4.2/1) mixture under static argon and nitrogen atmospheres ranging from 50 to 500 Torr. Laser-produced vapor plumes of about 0.5–1 cm long were generated under argon and nitrogen atmospheres between 200 and 500 Torr. Within this pressure range, the synthesized materials were collected as web-like filaments on the copper wire system. SEM and TEM studies on these samples reveal a very high yield of SWNT under both argon and nitrogen atmospheres [15]. Working below 200 Torr resulted in more diffuse plumes, which occasionally were very long. The produced material was collected as powder-like soot and contained very small amounts of SWNTs according to the former SEM and TEM studies. A similar result was obtained by other authors using the pulsed Nd:YAG laser ablation technique [16]. Amorphous carbon seems to dominate these samples independent of the used atmosphere. The evolution of the amount of SWNTs in the samples with pressure can be seen in the systematic intensity variation of the

Raman spectra presented in Fig. 6 for argon and nitrogen as buffer gas. For both kind of atmospheres, one clearly can observe from the low-frequency region (100–250 cm^{-1}) and as well from the high-frequency region (1500–1850 cm^{-1}) that the SWNT yield below 200 Torr drastically gets reduced and the spectra of the 50-Torr samples no longer show the typical SWNT signals. Furthermore, the evolution of the sharp peak structure around 1350 cm^{-1} in Fig. 6 to a broader structure typical for disordered carbon in the spectra below 200 Torr indicates the transition to sample material with higher contents of amorphous carbon. In Fig. 7 the pressure evolution is plotted for the peak located between 1584 and 1589 cm^{-1}. Here, the intensity of the peak for the 400-Torr argon sample is taken as reference value and set to 100%. The graph shows that the highest amounts of SWNTs (highest Raman intensities) are obtained within the pressure range of 200 to 400 Torr. At 100 Torr the signals are already drastically reduced and at 50 Torr no significant amount of SWNTs can be detected. No obvious difference in the pressure behavior of argon and nitrogen can be observed and in both cases similar sample quantities (only slightly lower for nitrogen) and qualities have been produced. This on first sight is surprising since the reactivity of argon and nitrogen is quite different and the formation of CN radicals [17, 18] as well as CN_x films [19, 20] in laser ablation of graphite targets under nitrogen atmospheres has been reported. In this case, the formation of both C−C and C−N would be more or less equally favored leading to an important decrease in the yield of SWNTs as a results of the competition between the growing carbon structures and the nitrogen molecules for the carbon species ejected during the ablation. Additionally, it was suspected that the incorporation of the C−N bonding in the SWNT network would inhibit the tube growth [21]. However, the results shown in this section suggest that also in nitrogen atmospheres under the pressure conditions employed in this work the C−C bonding formation and therefore the SWNTs growth is favored as also has been observed by Zhang et al. [21] in Nd:YAG laser ablation experiments.

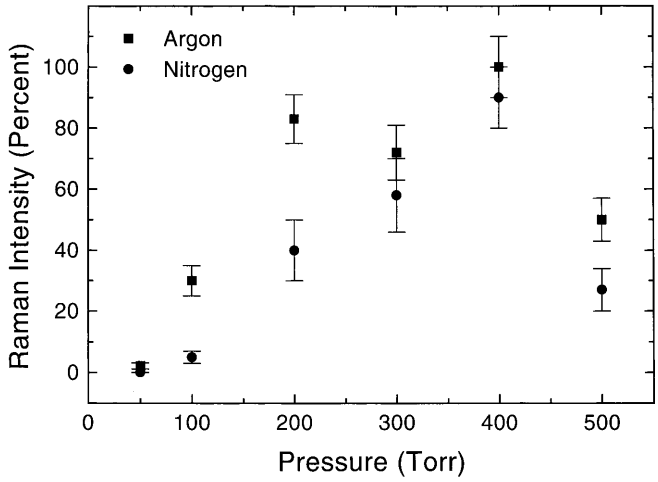

Fig. 7. Evolution of the Raman intensity of the high frequency peak located between 1584 and 1589 cm^{-1} with pressure for argon and nitrogen atmosphere. The intensity of the peak for the sample produced under 400 Torr of argon has been set to 100%

Finally, we should mention that no difference concerning quantity and quality has been observed performing experiments under either dynamic or static conditions. On the other hand, using helium as buffer gas and employing a pressure of 400 Torr, powder-like soot materials were produced. Like all other soot material having such a powder-like texture, these contained only negligible amounts of SWNTs as could be seen in SEM/TEM and Raman studies.

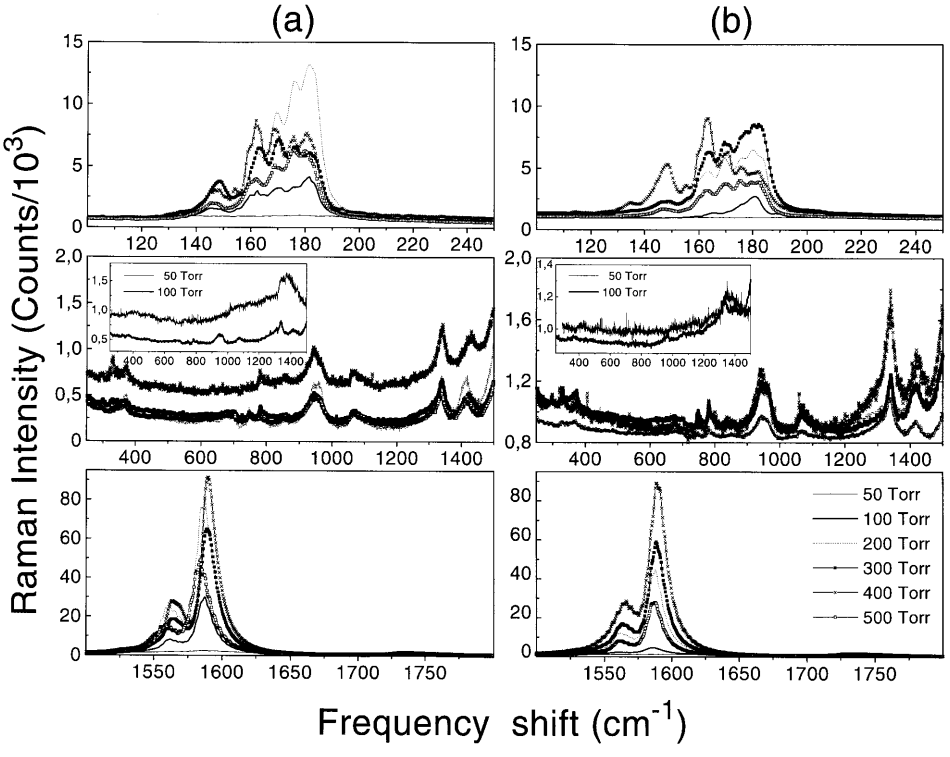

Fig. 6a,b. Raman spectra of SWNT material produced with a Ni/Y (4.2/1 at %) under different pressures in **a** argon and **b** in nitrogen atmospheres. The *top of the figures* represents the low-frequency range from 100 to 250 cm^{-1}, the middle of the figures shows the intermediate-frequency region from 250 to 1500 cm^{-1}, and the lower part of the figure displays the high-frequency range from 1500 to 1850 cm^{-1}

The understanding of the described pressure and gas effects can be related to changes of the local temperature environment experienced by the evaporated species close to the target rod. This will be explained in the next section.

2.3 Influence of the local temperature

The 10.6-μm cw laser radiation is able to induce favorable conditions for the SWNT growth by evaporating material from the graphite/metal-composite targets and, simultaneously, inducing a hot zone of about 1 cm around the focal spot on the target. In this orange-red zone temperatures around 1200 °C were measured when operating at 400 Torr under argon atmospheres. The hot rod itself acts as a local furnace and reduces the temperature gradient experienced by the evaporated species. This helps to keep the environment at temperatures suitable for the growth of SWNTs without the use of an external furnace. It becomes clear that this system allows efficient laser–target–gas interactions and therefore shows that the local conditions, i.e. especially the temperature and the temperature gradient near the evaporation zone, play an important role in the formation process of SWNTs. These assumptions seem to be further confirmed by the results of Kokai et al. [22] who used a pulsed CO_2-laser system. The fact that here high yields of SWNT ($> 60\%$) only were obtained using an external furnace clearly shows that in a pulsed mode the target rod apparently is not continuously heated for establishing the favorable local temperature environment as is the case when working in cw-mode conditions.

The gas and pressure effects described above can be directly related to the change of these local conditions. Since lighter gases are more efficient for rapid cooling than heavier ones (inverse proportional to the square root of the molecular weight) the temperature gradient, i.e. cooling rate experienced by the evaporated species, becomes too large to favor the SWNT formation [9, 23]. This certainly is the case when helium is used as buffer gas, which has a much lower molecular weight than argon and nitrogen. On the other hand, the temperature gradients created under the studied nitrogen atmospheres were still small enough to provide SWNT yields comparable to those obtained under argon.

The influence of the gas pressure on the SWNT formation also is closely related to the local temperature effects. A pressure between 200 and 400 Torr restricts the expansion of the vapor plume (confinement effect) and by avoiding excessive cooling, high yields of SWNTs can be produced. However, under low pressures, the vapor plume will expand too rapidly (as indicated by the longer vapor plumes in experiments below 200 Torr) leading to an increased cooling rate for the evaporated species which finally results in a decreased production of SWNTs. On the other hand, increased pressures (beyond 400 Torr) will result in too high collision probabilities of the evaporated species with the ambient gas molecules and therefore leads as well to increased cooling rates which reduce the efficiency of SWNT formation. Finally it should be mentioned that besides an influence on the local temperature conditions the gas pressure could also have an effect on the local concentration of evaporated carbon and metal species.

3 Conclusion

The simple cw CO_2-laser ablation technique described in this work is able to provide high yields of SWNTs under a relatively wide range of experimental conditions. It has been shown that the target composition, the buffer gas, and the gas pressure are influencing particularly the quantity of the produced SWNT material but also the characteristics of the SWNT itself. In general, bi-metal mixtures such as Ni/Y and Ni/Co yielded the largest amounts of SWNT material. The use of different mixtures can also have an effect on the diameter distribution, however no clear correlation could be established. The microscopic details concerning the role of the metal particles still remain unclear. On the other hand, the effects of the buffer gas and the gas pressure on the yield of SWNTs can be directly related to changes of the local temperature environment near the evaporation zone. It therefore becomes clear that the use of certain metals or metal combination in the graphite targets, its concentration in the gas phase, and the local temperature conditions play a key role in the formation of SWNTs. This should be independent of any applied technique based on the evaporation of graphite/metal targets.

Finally it is worth noting that the cw CO_2-laser ablation technique presented here is a simple but efficient method for the production of SWNTs. Since this type of laser is already widely used in industry, automating this system will be a mayor step forward towards the mass production of SWNTs.

Acknowledgements. This work was supported by the DGICYT (Project PB94-0224). E.M. acknowledges funding from the Departamento de Educación y Cultura de la Comunidad Autónoma de Aragón.

References

1. S.J. Tans, M.H. Devoret, H. Dai, A. Thess, R.E. Smalley, L.J. Geerligs, C. Dekker: Nature **386**, 474 (1997)
2. S. Frank, Ph. Poncharal, Z.L. Wang, W.A. de Heer: Science **280**, 1744 (1998)
3. B.I. Yacobson, R.E. Smalley: American Scientist **85**, 324 (1997)
4. A.C. Dillon, K.M. Jones, T.A. Bekkedahl, C.H. Kiang, D.S. Bethune, M.J. Heben: Nature **386**, 377 (1997)
5. C. Journet, W.K. Maser, P. Bernier, A. Loiseau, M. Lamy de la Chapelle, S. Lefrant, P. Deniard, R. Lee, J.E. Fischer: Nature **388**, 756 (1997)
6. A. Thess, R. Lee, P. Nikolaev, H. Dai, P. Petit, J. Robert, C. Xu, Y.H. Lee, S.G. Kim, A.G. Rinzler, D.T. Colbert, G.E. Scuseria, D. Tománek, J.E. Fischer, R.E. Smalley: Science **273**, 483 (1996)
7. A.G. Rinzler, J. Liu, H. Dai, P. Nikolaev, C.B. Huffman, F.J. Rodríguez-Macías, P.J. Boul, A.H. Lu, D. Heymann, D.T. Colbert, R.S. Lee, J.E. Fischer, A.M. Rao, P.C. Eklund, R.E. Smalley: Appl. Phys. A **67**, 29 (1998)
8. W.K. Maser, E. Muñoz, A.M. Benito, M.T. Martínez, G.F. de la Fuente, Y. Maniette, E. Anglaret, J.L. Sauvajol: Chem. Phys. Lett. **292**, 587 (1998)
9. E.G. Gamaly, A.V. Rode, W.K. Maser, E. Muñoz, A.M. Benito, M.T. Martínez, G.F. de la Fuente: Appl. Phys. A, DOI 10.1007/s003390000254
10. G.S. Duesberg, J. Muster, V. Krstic, M. Burghard, S. Roth: Appl. Phys. A **67**, 117 (1998)
11. T. Guo, P. Nikolaev, A. Thess, D.T. Colbert, R.E. Smalley: Chem. Phys. Lett. **243**, 49 (1995)
12. Y. Saito: Carbon **33**, 979 (1995)
13. S. Bandow, S. Asaka, Y. Saito, A.M. Rao, L. Grigorian, E. Richter, P.C. Eklund: Phys. Rev. Lett. **80**, 3779 (1998)

14. S. Rols, A. Righi, L. Álvarez, E. Anglaret, C. Journet, P. Bernier, J.L. Sauvajol, A.M. Benito, W.K. Maser, E. Muñoz, M.T. Martínez, G.F. de la Fuente, A. Girard, J.C. Ameline: unpublished
15. E. Muñoz, W.K. Maser, A.M. Benito, M.T. Martínez, G.F. de la Fuente, Y. Maniette, A. Righi, E. Anglaret, J.L. Sauvajol: Carbon, unpublished
16. M. Yudasaka, T. Komatsu, T. Ichihashi, Y. Achiba, S. Iijima,: J. Phys. Chem. B **102**, 4892 (1998)
17. J. Hermann, C. Vivien, A.P. Carricato, C. Boulmer-Leborgne: Appl. Surf. Sci. **127-129**, 645 (1998)
18. G. Dinescu, E. Aldea, M.L. De Giorgi, A. Luches, A. Perrone, A. Zocco: Appl. Surf. Sci. **127-129**, 697 (1998)
19. Y. Suda, T. Nakazono, K. Ebihara, K. Baba, S. Aoqui: Carbon **36**, 771 (1998)
20. C. Jama, P. Goudmand: Carbon **36**, 785 (1998)
21. Y. Zhang, H. Gu, S. Iijima: Appl. Phys. Lett. **73**, 3827 (1998)
22. F. Kokai, K. Takahashi, M. Yudasaka, R. Yamada, T. Ishihashi, S. Iijima: J. Phys. Chem. B **103**, 4346 (1999)
23. S.S. Harilal, C.V. Bindhu, V.P.N. Nampoori, C.P.G. Vallabhan: Appl. Phys. Lett. **72**, 167 (1998)